

AD-A210 510

ADVANCED DOUBLE LAYER CAPACITOR

Prepared by:

Anthony B. LaConti, Ph.D.  
Philip Lessner, Ph.D.  
S. Sarangapani, Ph.D.

GINER, INC.  
14 Spring Street  
Waltham, MA 02254-9147  
(617)899-7270

July, 1989

3rd Quarter Interim Technical Report

November 1, 1988 to January 31, 1989

Contract No. N00014-88-C-0391  
ARPA Order No. 9526

DTIC  
ELECTE  
JUL 26 1989  
S D & D

Prepared For:

OFFICE OF NAVAL RESEARCH  
Department of the Navy  
800 N. Quincy Street  
Arlington, Virginia 22217

**DISTRIBUTION STATEMENT A**

Approved for public release  
Distribution Unlimited

*The views and conclusions contained in this document are those of the authors and should not be interpreted as necessarily representing the official policies, either expressed or implied, of the Defense Advanced Research Projects Agency or the U.S. Government.*

**THIS DOCUMENT HAS BEEN APPROVED FOR PUBLIC RELEASE AND SALE.  
ITS DISTRIBUTION IS UNLIMITED WITH THE EXCEPTION OF THE APPENDIX  
WHICH IS LIMITED TO GOVERNMENT PERSONNEL.**

89 . 7 26 041

GINER, INC.

14 SPRING STREET • WALTHAM, MASSACHUSETTS 02254-9147 • (617) 899-7270

# TABLE OF CONTENTS

|  |    |
|--|----|
| TABLE OF CONTENTS .....  | i  |
| LIST OF FIGURES .....  | ii |
| 1. TECHNICAL OBJECTIVES .....  | 1  |
| 2. EXPERIMENTAL METHODS .....  | 1  |
| 2.1 Preparation and Characterization of RuO <sub>x</sub> Powders ..... | 1  |
| 2.1.1 Preparation .....  | 1  |
| 2.1.2 Surface Area .....   | 1  |
| 2.1.3 X-Ray Diffraction .....  | 2  |
| 2.1.4 Scanning Electron Microscopy .....                               | 2  |
| 2.2 Preparation of Membrane and Electrode Assemblies .....             | 2  |
| 2.3 Electrode Testing .....  | 3  |
| 2.3.1 Cell Design .....  | 3  |
| 2.3.2 Cyclic Voltammetry .....   | 3  |
| 2.3.3 AC Impedance .....   | 3  |
| 3. RESULTS AND DISCUSSION .....  | 3  |
| 3.1 Characterization of RuO <sub>x</sub> .....                         | 3  |
| 3.2 Electrode Characterization .....                                   | 5  |
| 3.2.1 Cell Design .....  | 5  |
| 3.2.2 M and E Testing .....  | 8  |
| 3.2.3 AC Impedance .....   | 14 |
| 4. FUTURE WORK .....   | 18 |



|           |  |
|-----------|--|
| by        |  |
| Date      |  |
| Approved  |  |
| Signature |  |
| A-1       |  |

## LIST OF FIGURES

|           |  |    |
|-----------|--|----|
| Figure 1  | Test Fixture for Liquid Electrolyte-Free Capacitor Cell .....                                | 4  |
| Figure 2  | SEM Photograph of RuO <sub>2</sub> Particulates .....  | 6  |
| Figure 3  | Powder X-Ray Diffraction Patterns of RuO <sub>x</sub> Made by Thermal Method .....           | 7  |
| Figure 4  | Voltammograms and Current Density vs. Sweep Rate Plots for RuO <sub>x</sub> Electrodes ..... | 9  |
| Figure 5  | Voltammograms and Current Density vs. Sweep Rate Plots for RuO <sub>x</sub> Electrodes ..... | 10 |
| Figure 6  | Voltammograms and Current Density vs. Sweep Rate Plots for RuO <sub>x</sub> Electrodes ..... | 11 |
| Figure 7  | Voltammograms and Current Density vs. Sweep Rate Plots for RuO <sub>x</sub> Electrodes ..... | 12 |
| Figure 8  | Voltammograms and Current Density vs. Sweep Rate Plots for RuO <sub>x</sub> Electrodes ..... | 13 |
| Figure 9  | Nyquist Plot for RuO <sub>x</sub> on a Ti Disk .....   | 15 |
| Figure 10 | Nyquist Plot for Equivalent Circuit .....  | 15 |
| Figure 11 | Nyquist Plot for Ferri/Ferro Cyanide Couple .....  | 16 |
| Figure 12 | Impedance of Ferri/Ferro Cyanide System .....  | 16 |
| Figure 13 | Nyquist Plot; RuO <sub>x</sub> on Ti Disk of 3 mm Diameter .....                             | 17 |

## 1. TECHNICAL OBJECTIVES

The overall goal of this project is to develop electrochemical capacitors with no liquid electrolyte present. The liquid electrolyte is replaced by a solid ionomer electrolyte. An advantage of these devices over conventional electrochemical capacitors containing free acid would be greater safety and reliability.

In the third quarter, we concentrated our efforts in three areas: 1) preparation and characterization of  $\text{RuO}_x$  powders, 2) preparation of membrane and electrode (M and E) assemblies with high capacitance, and 3) AC impedance characterization of M and E assemblies.

## 2. EXPERIMENTAL METHODS

### 2.1 Preparation and Characterization of $\text{RuO}_x$ Powders

#### 2.1.1 Preparation

Preparation of  $\text{RuO}_x$  by the thermal method was done as reported in the 2<sup>nd</sup> Quarterly Report.

#### 2.1.2 Surface Area

One of the key parameters to control for the particulate electrode materials used in electrochemical capacitors is surface area. The surface area of a sample can be related to the adsorption of a monolayer of gas by:

$$S = \frac{V_m AN}{M} \quad [1]$$

where  $S$  is the surface area,  $V_m$  is the volume of monolayer,  $A$  is Avogadro's number,  $N$  is the surface area of the adsorbed gas molecule, and  $M$  is the molar volume of the gas. The relationship between the volume of gas adsorbed  $V$  and the monolayer volume,  $V_m$  is given by the BET equation:

$$(P/P_0)/V[1 - (P/P_0)] = 1/(V_m C) + [(C - 1)/(V_m C)]P/P_0 \quad [2]$$

where  $V$  is the volume (at STP) of adsorbed gas at pressure  $P$ ,  $P_0$  is the vapor pressure of the gas at the adsorbing temperature, and

C is a constant related to the energy of adsorption. Since  $C \gg 1$  and  $P/P_0 \gg 1/C$ , the BET equation can be simplified to:

$$V_m = V[1 - (P/P_0)] \quad [3]$$

which can be substituted into Equation 1 to yield:

$$S = VAN[1 - (P/P_0)]/M \quad [4]$$

from which the surface area can be obtained once the volume of gas, V, is measured and appropriate values for the other terms are incorporated. The specific surface area ( $m^2/g$ ) is obtained by dividing the surface area by the mass of the sample.

Surface areas were measured using a Micromeritics Flowsorb II 2300 apparatus. The adsorbing gas has 30 mole%  $N_2$  in He at liquid  $N_2$  temperature. A measurement of V was made using the apparatus and surface areas were calculated using Equation 4.

### 2.1.3 X-Ray Diffraction

X-ray diffraction can be used to identify oxide and impurity phases and crystallite sizes. Powder X-ray diffraction was done by E.S. Laboratories (Wrightstown, NJ).

### 2.1.4 Scanning Electron Microscopy

Scanning electron microscopy (SEM) was used to study particle size and morphology. SEM work was done at Eastern Analytical Laboratories (Billerica, MA).

## 2.2 Preparation of Membrane and Electrode Assemblies

The Nafion electrolyte was introduced into the electrode by two different methods: 1) mixing of the Nafion solution with the  $RuO_2$  powder followed by evaporation of the solvent and then fabrication of the resulting composite into an electrode and 2) impregnation of an already formed Teflon-bonded  $RuO_2$  electrode with a Nafion solution followed by evaporation of the solvent.

The resulting electrodes are bonded to a Nafion 117 membrane using a moderate temperature pressing procedure. The M and E assembly is rehydrated after pressing.

## 2.3 Electrode Testing

### 2.3.1 Cell Design

This quarter we have made the transition from testing in cells where the outer face of the M and E was in contact with 1M H<sub>2</sub>SO<sub>4</sub> to cells where no H<sub>2</sub>SO<sub>4</sub> is present (liquid electrolyte-free cell). The new test cell is shown in Figure 1. The M and E is held between two acrylic plates. To keep the M and E wet, a water reservoir is in contact with the edge of the M and E. Contact to the M and E is made via Au-plated brass leads (a Au-plated Ti backing plate placed in back of the M and E prevents the leads from puncturing the membrane). The ionomer membrane has a tail which can dip into a beaker of H<sub>2</sub>SO<sub>4</sub> containing a Hg/HgSO<sub>4</sub> reference electrode. Some M and Es are made with integrally bonded Pt/air reference electrodes.

### 2.3.2 Cyclic Voltammetry

Cyclic voltammetry continued to be the principle means of characterizing M and E structures for their effective capacitance. A repetitive, linear potential sweep was applied in the region of -0.4 to 0.5 V vs. Hg/HgSO<sub>4</sub> (which was determined to be a region where only capacitive and surface redox processes were occurring). The current at +0.1 V was plotted against sweep rate and the capacitance determined using:

$$C = \frac{i}{(dv/dt)} \quad [5]$$

### 2.3.3 AC Impedance

The instrumentation was the same as described in the 2nd Quarterly Technical Report.

## 3. RESULTS AND DISCUSSION

### 3.1 Characterization of RuO<sub>x</sub>

During the 3<sup>rd</sup> Quarter, the RuO<sub>x</sub> powder made by the thermal method has been characterized by scanning electron microscopy (SEM), X-ray diffraction (XRD), and N<sub>2</sub> adsorption surface area measurements (BET). Electrodes made from the powder have been examined using SEM and BET.

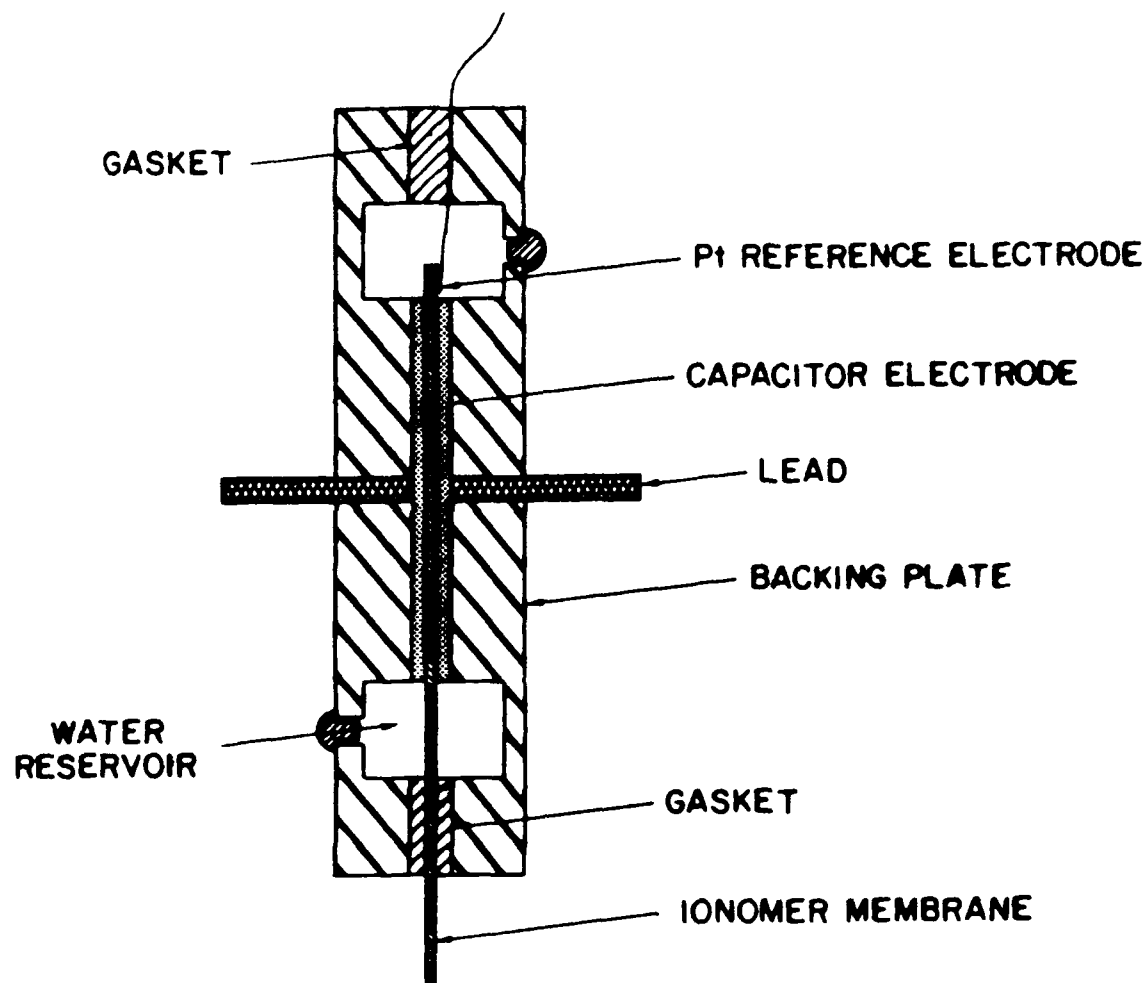


Figure 1: Test Fixture for Liquid Electrolyte-Free Capacitor Cell.

A SEM of the powder is shown in **Figure 2**. Several submicron size particles as well as micron size particles and larger clumps of particles can be seen. At the magnifications accessible with the SEM, no internal porosity can be detected. Some of the particles appear to be prismatic in shape.

Specific surface areas for the powders measured by the BET method have ranged from 18-50 m<sup>2</sup>/g, if the powder was not heat treated after preparation. Assuming spherical particles,  $d_p = 6/dS_g$ , where  $d$  is the density of RuO<sub>x</sub> and  $S_g$  is the specific surface area. This gives average particles sizes ranging from 170-480 Å. This is considerably smaller than the particles and aggregates observed using SEM, indicating that the RuO<sub>x</sub> particles may be made up of grains too small to see with the SEM. A Teflon-bonded electrode made from 50 m<sup>2</sup>/g RuO<sub>x</sub> particulates had a surface area of 25 m<sup>2</sup>/g.

The X-ray diffraction pattern obtained from the RuO<sub>x</sub> powder is shown in **Figure 3**. The peaks correspond to those of RuO<sub>2</sub>. Peak widths indicate that there are two groupings of crystallite sizes - about 1 μm and a much smaller size as well.

Based on the results of X-ray diffraction measurements, the RuO<sub>x</sub> prepared by the thermal method at 550°C appears to be almost pure RuO<sub>2</sub>. SEM examination shows that the aggregate size of the particulates is on the order of 1 μm. However, the surface area measurements suggest that these aggregates are made up of crystallites of much smaller size. The use of transmission electron microscopy (TEM) would be needed to see the morphology of these smaller crystallites.

### **3.2 Electrode Characterization**

#### **3.2.1 Cell Design**

The test cell used in experiments during the first two quarters consisted of a holder for the membrane and electrode assembly (M and E) dipping into a sulfuric acid solution. The reference electrode and counter electrode are in the sulfuric acid solution. It was hoped that this arrangement would allow quick screening of different electrode-ionomer composite structures.





Figure 2: SEM Photograph of RuO<sub>2</sub> Particulates.

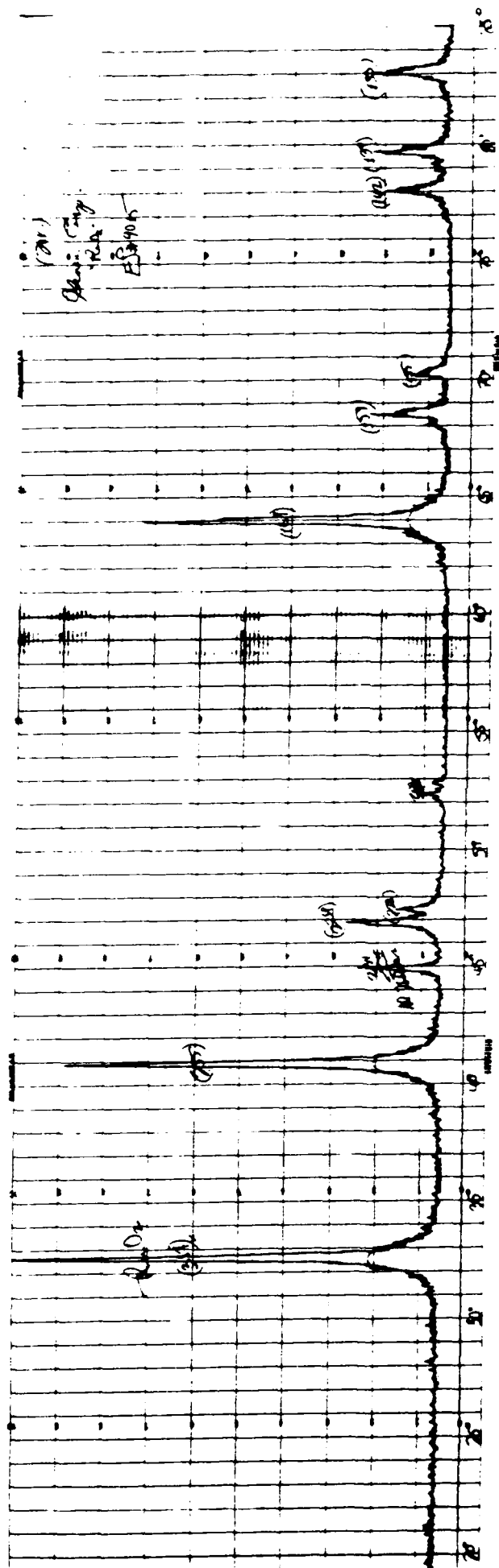


Figure 3: Powder X-Ray Diffraction Patterns of  $\text{RuO}_4$  Made by Thermal Method.

Figures 4 and 5 compare the results obtained with a nonimpregnated  $\text{RuO}_x$  bonded to a Nafion membrane and a nonimpregnated  $\text{RuO}_x$  with no Nafion membrane. Both were tested with one face in contact with 1M  $\text{H}_2\text{SO}_4$ . The electrode with no Nafion membrane should be completely flooded. The capacitance is  $1.37 \text{ F/cm}^2$ . If the electrode with the membrane was liquid electrolyte free (the only electrode-electrolyte contact would be at the  $\text{RuO}_x$ -Nafion interface), then its capacitance should be much lower. In fact, its capacitance is  $1.43 \text{ F/cm}^2$ , which shows that substantial  $\text{H}_2\text{SO}_4$  has been imbibed into the electrode pores. Figure 6 shows for comparison an M and E tested in the dry cell. Its capacitance is  $0.101 \text{ F/cm}^2$ , which is an order of magnitude lower than the similar electrode tested in the wet cell.

Sulfuric acid is most likely transported through the Nafion membrane by diffusion (the membrane is not a perfect rejecter of anions). This, coupled with electroosmotic transport of water, allows some liquid electrolyte to permeate into the structure, which causes partial flooding. On the basis of these results, we made the decision to switch to the dry cell.

### 3.3.2 M and E Testing

When tested in the liquid electrolyte-free cell with no Nafion in the bulk of the electrode structure, the M and E's show capacitances of 0.1 to  $0.2 \text{ F/cm}^2$  (Figure 6). Figure 7 shows the result when 10 wt% Nafion (as a solution of Nafion 117) was mixed with the  $\text{RuO}_x$  powder. The solvent was then allowed to evaporate and the resulting composite powder was crushed and then fabricated into an electrode, which was bonded to a Nafion 117 membrane to form an M and E. The resulting M and E did not have a significantly higher capacitance than the M and E's which were made with no Nafion in the bulk of the electrode structure.

As another approach to forming a three dimensional interface, Teflon-bonded  $\text{RuO}_x$  electrodes were impregnated with a Nafion 117 solution. Adding the solution via a dropper to the face of the electrode produced electrodes covered with a Nafion film with little evidence that Nafion had actually penetrated into the electrode structure. To draw the Nafion into the bulk electrode, the electrodes were impregnated under a vacuum. Figure 8 shows that a somewhat higher capacitance of  $0.342 \text{ F/cm}^2$  was obtained than in the base case with no impregnation.

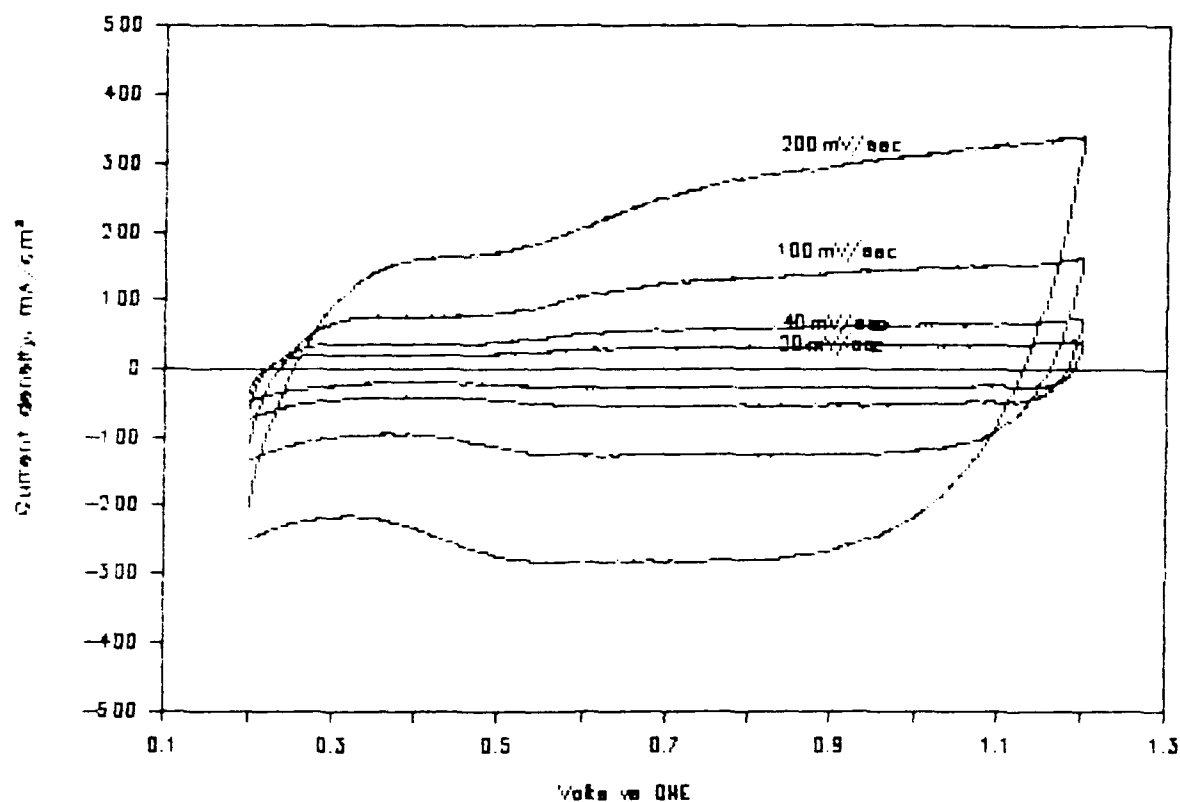


Figure 4a. Voltammograms of  $\text{RuO}_x$  Electrodes ( $22.7 \text{ mg/cm}^2$  Loading) Flooded with  $1\text{M H}_2\text{SO}_4$ .

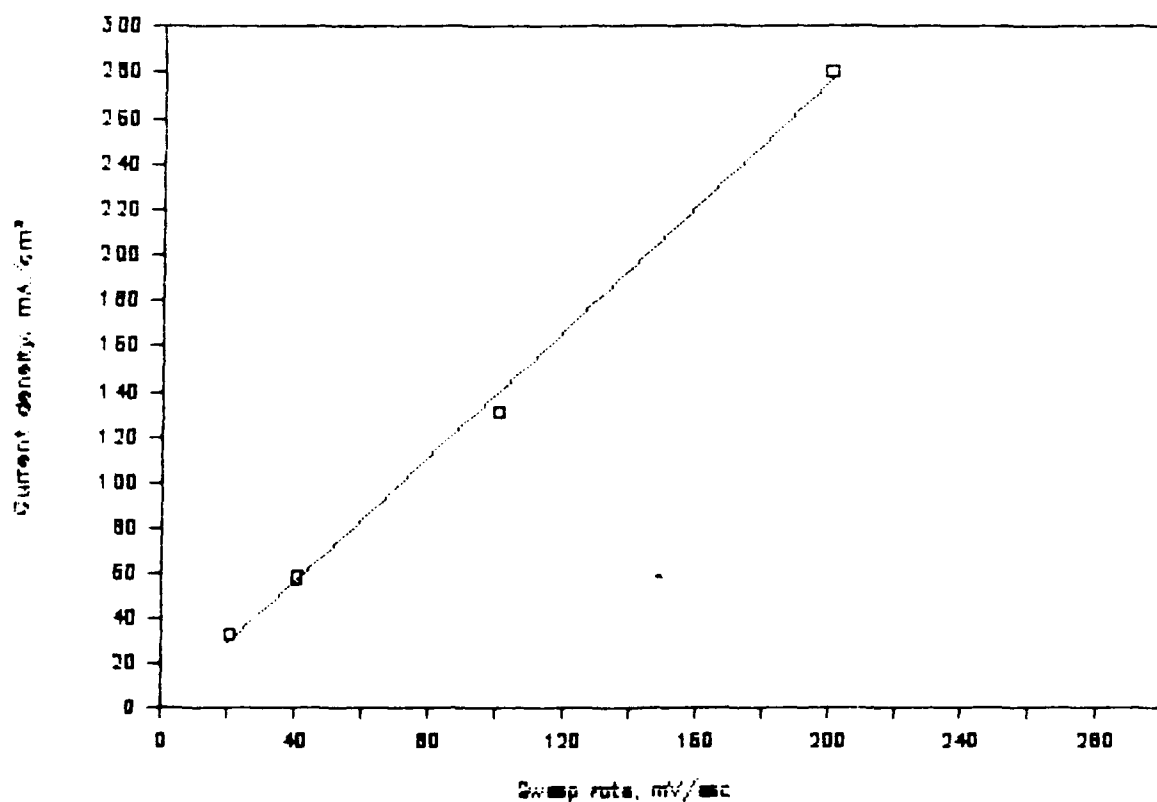


Figure 4b. Current Density vs. Sweep Rate. The Calculated Capacitance is  $1.37 \text{ F/cm}^2$ .

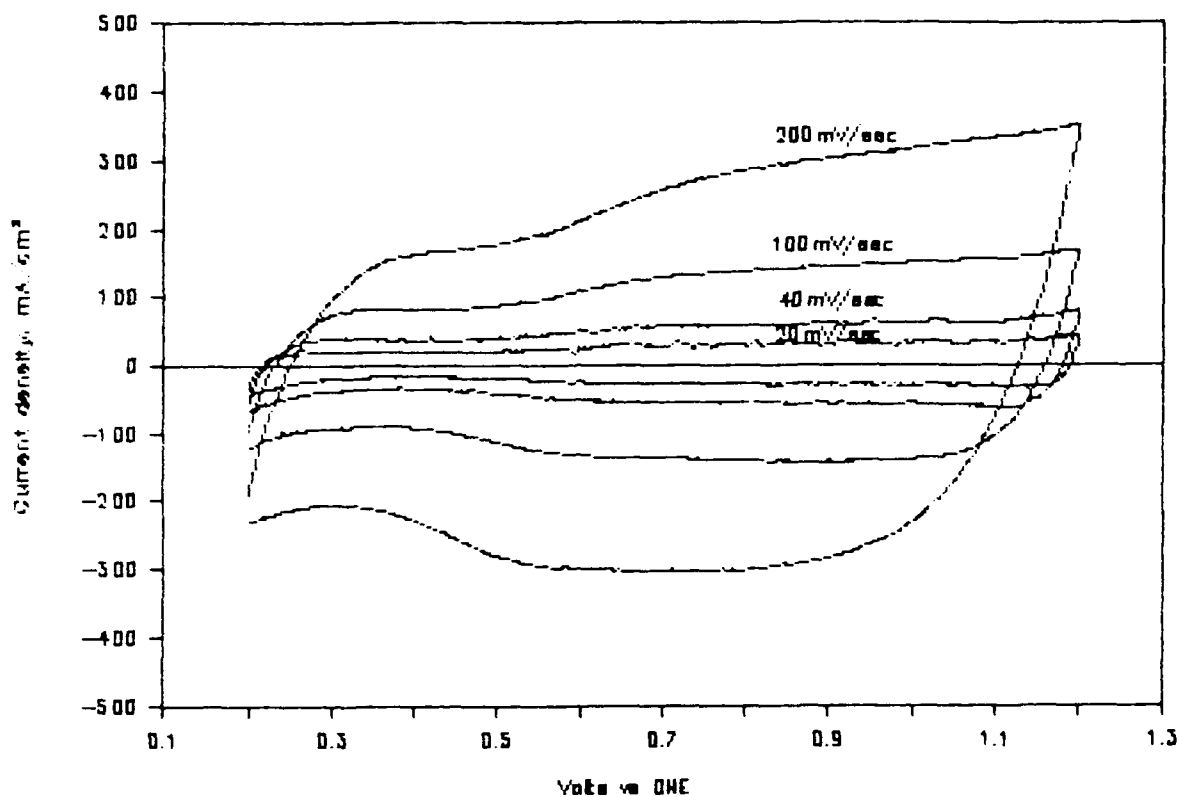


Figure 5a. Voltammograms of  $\text{RuO}_x$  Bonded to Nafion Membrane. The outer face of the membrane was in contact with  $1\text{M H}_2\text{SO}_4$ .

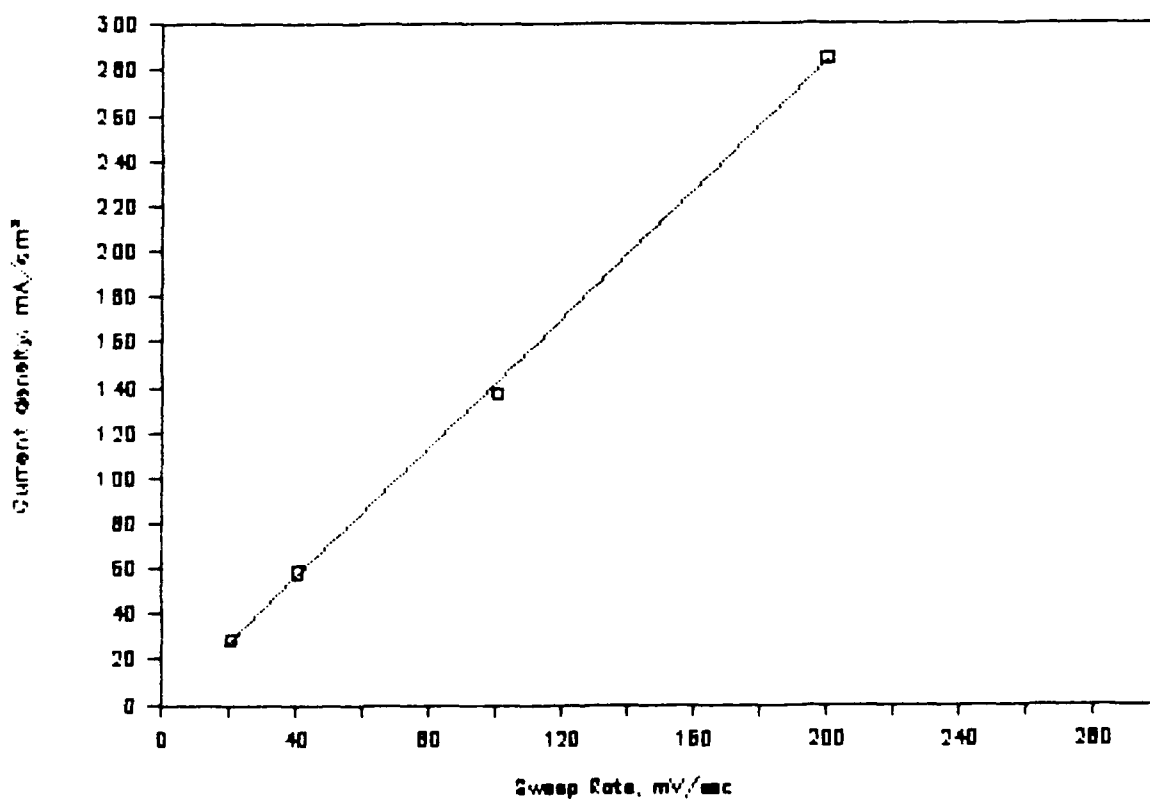


Figure 5b. Current Density vs. Sweep Rate. The Calculated Capacitance is  $1.43 \text{ F/cm}^2$ .

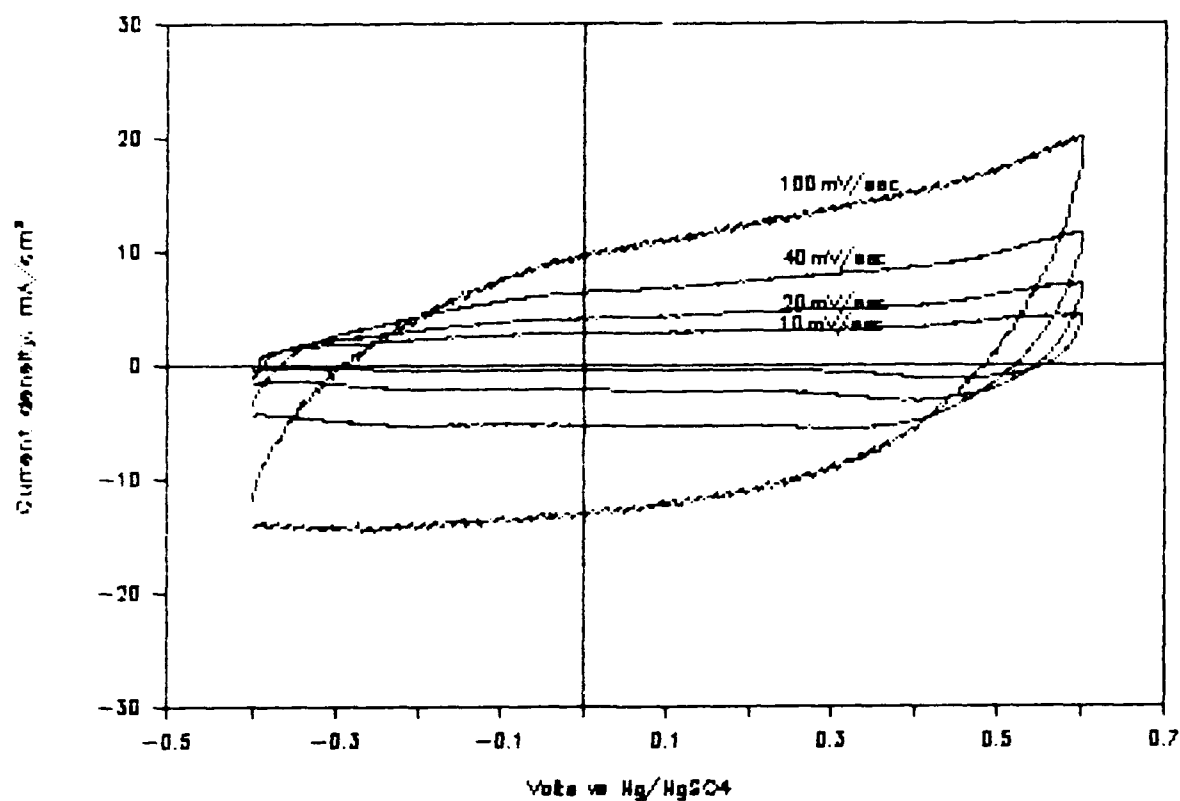


Figure 6a. Voltammograms of RuO<sub>x</sub> Bonded to Nafion Membrane (15 mg/cm<sup>2</sup> Loading); Tested in Cell of Figure 1.

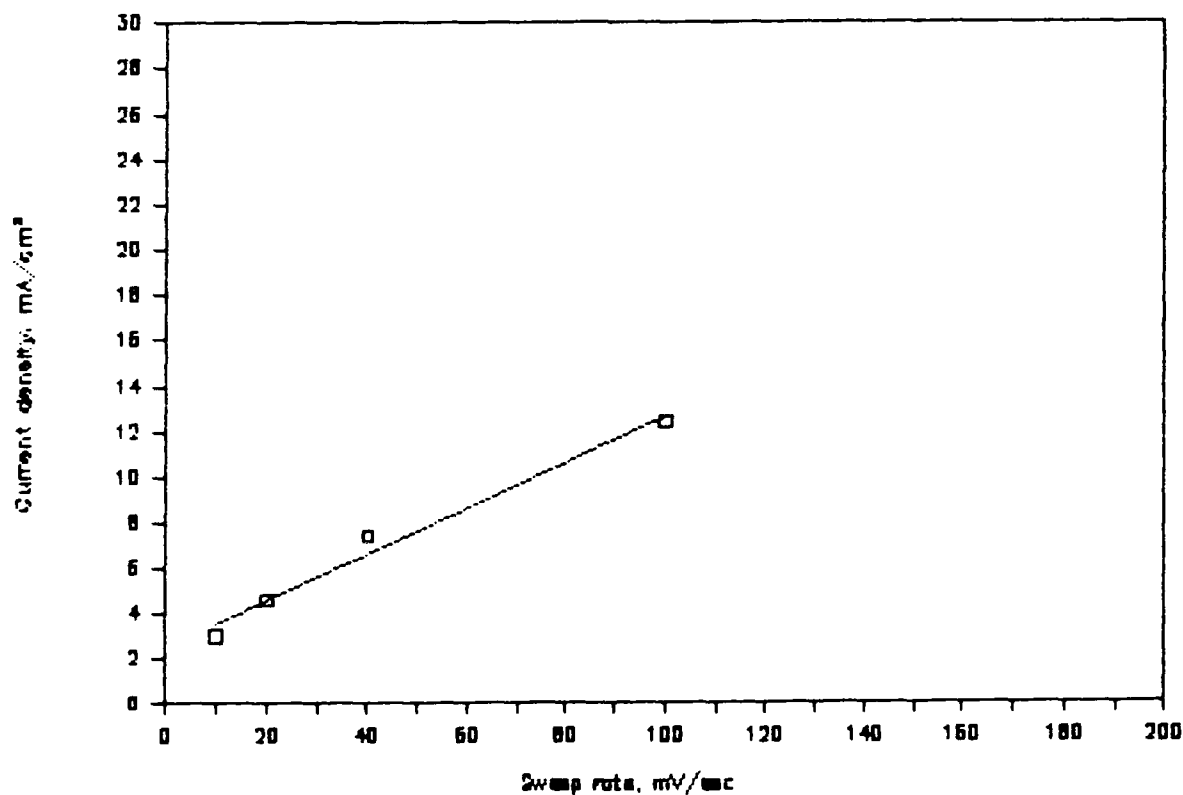


Figure 6b. Current Density vs. Sweep Rate. The Calculated Capacitance is 0.101 F/cm<sup>2</sup>.

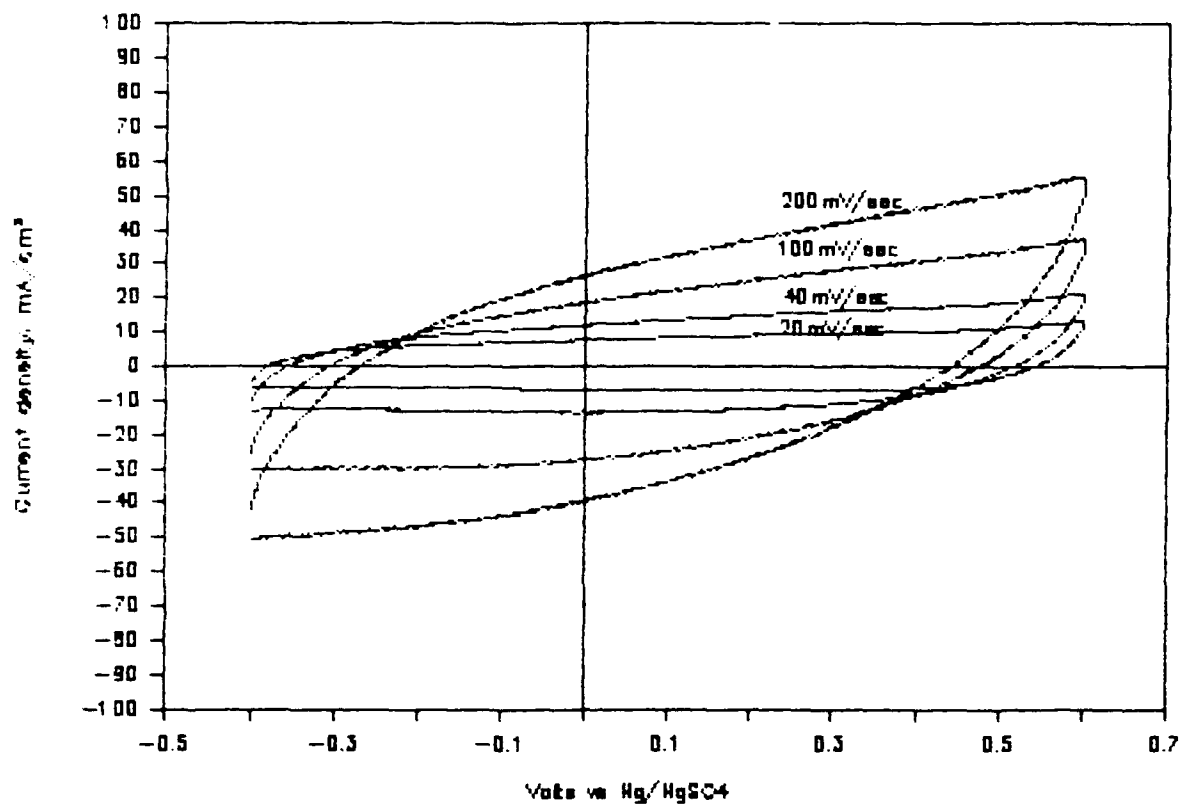


Figure 7a. Voltammograms of RuO<sub>x</sub> Bonded to Nafion Membrane. RuO<sub>x</sub> was mixed with 10 wt% Nafion solution; Tested in Cell of Figure 1.

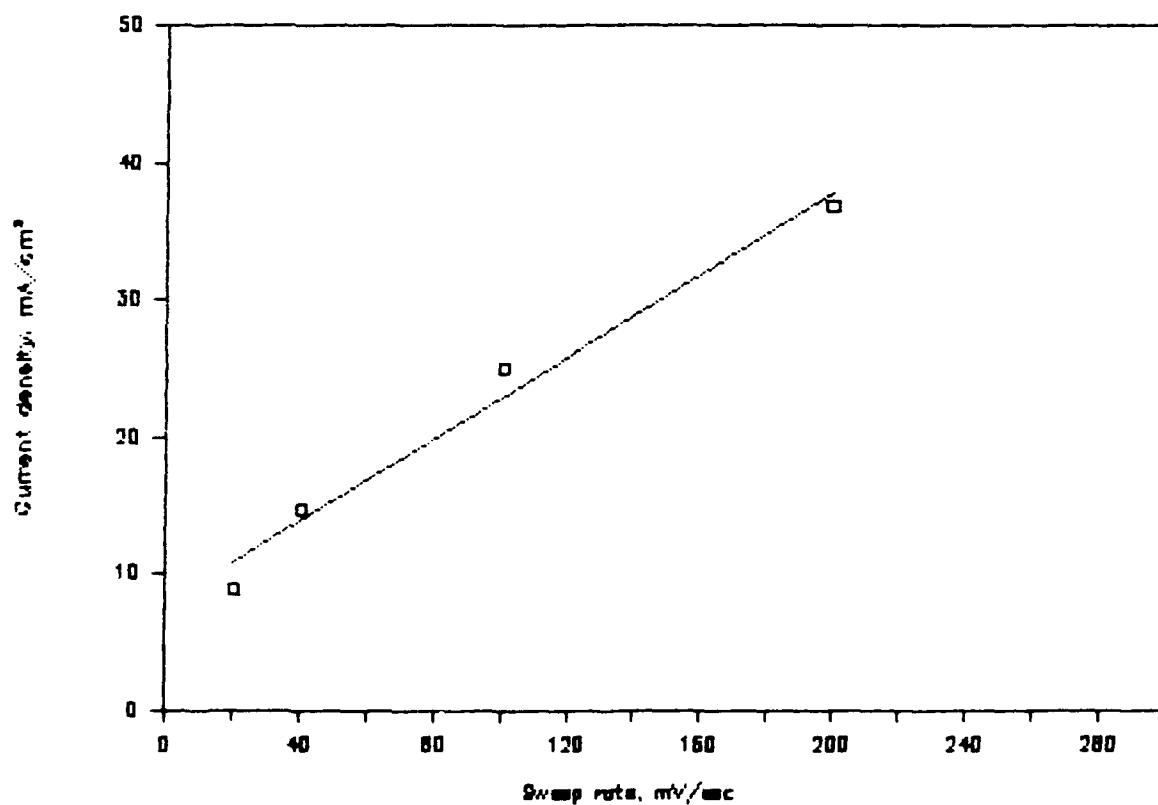


Figure 7b. Current Density vs. Sweep Rate. The Calculated Capacitance is 0.149 F/cm².

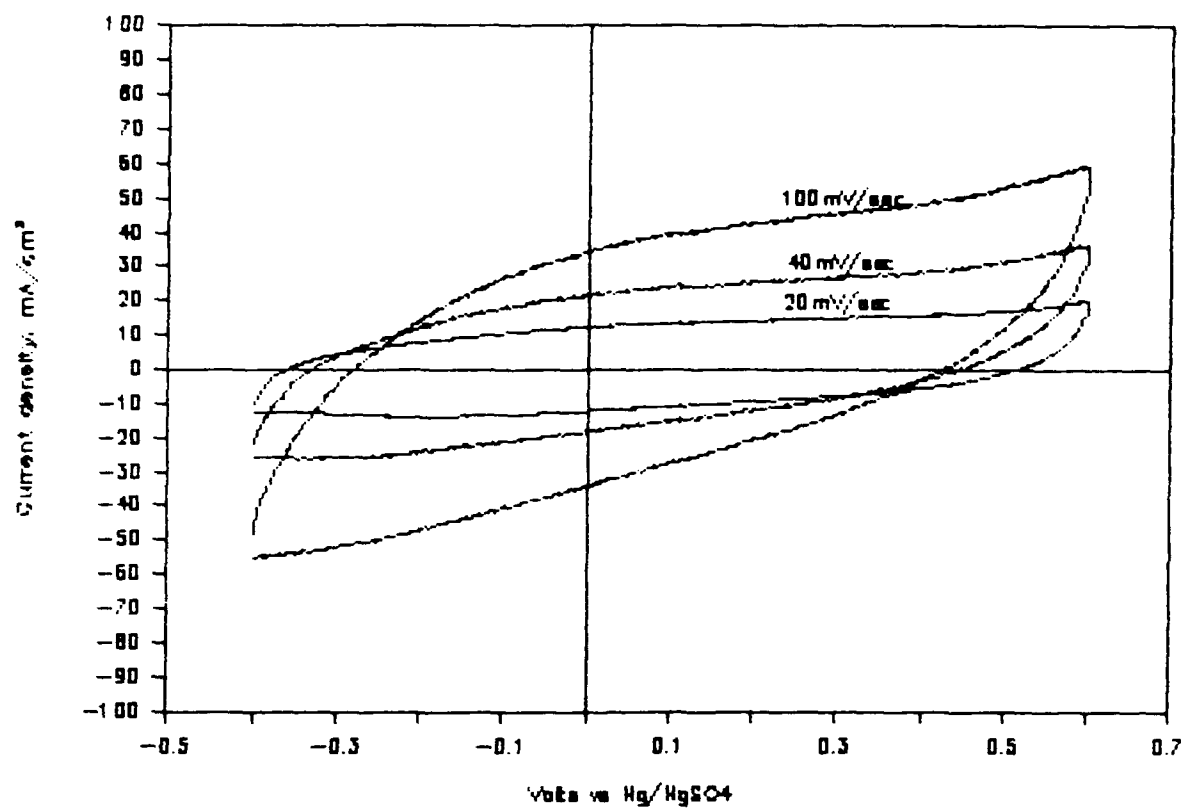


Figure 8a. Voltammograms of RuO<sub>x</sub> Vacuum Impregnated with Nafion and Pressed Against a Nafion Membrane; Tested in Cell of Figure 1.

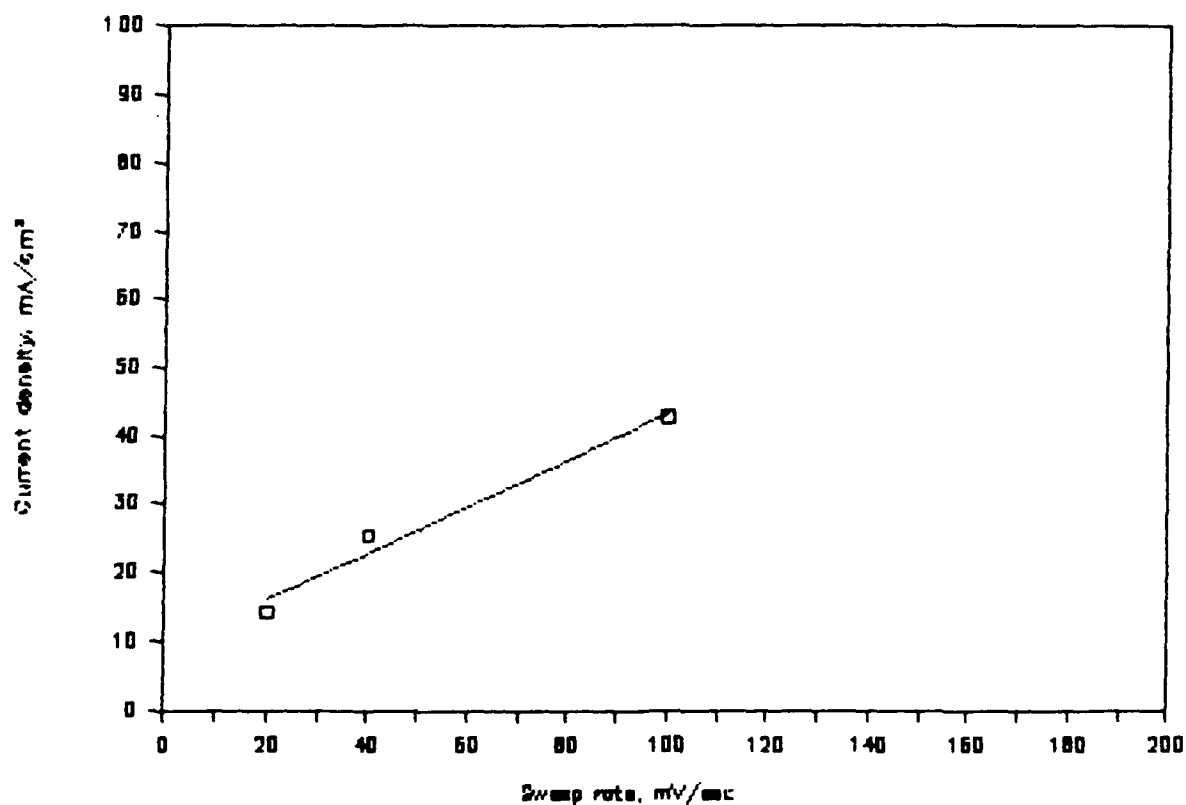


Figure 8b. Current Density vs. Sweep Rate. Calculated Capacitance is 0.342 F/cm<sup>2</sup>



### 3.2.3 AC Impedance

In the last quarter, we reported on a setup to measure impedances based on the PAR5210 lock-in amplifier and PAR 173/276 potentiostat. During this quarter, we further developed the method to see whether we can use this method to qualify the M and Es. The following is a summary of our findings:

Figure 9 shows the impedance of a  $\text{RuO}_x$  sprayed onto a titanium disk. The reactive part of the impedance is only 0.4 ohm and the real part -4 ohms. The inductive reactance values beyond 1000 Hz, are of the same order as the capacitive reactance. Since the frequency at which the inductance appeared was very low, we investigated a test circuit (20  $\mu$ F in parallel with 50 KSV) up to a frequency of 100 kHz (Figure 10). The inductive reactance in this case did not appear until we reached a frequency of 30 kHz. Our initial suspicion was therefore on the electrochemical cell and naturally the reference electrode with its high impedance was the prime suspect. Figure 11 shows an impedance spectrum obtained with the same  $\text{RuO}_x$  electrode as in Figure 9, but with a low impedance  $\text{IrO}_x$  reference electrode and a large platinized platinum counter electrode. The impedance data obtained with this experimental arrangement is no better.

In order to validate the electrochemical cell and instrumentation, we proceeded to obtain data on the standard ferri/ferro cyanide couple. Figure 12 shows the data; the reactance does not become inductive until we reach a frequency of 8 kHz. Although this is not a very good result, the high frequency limit of 8 kHz was encouraging. Closer examination of the data revealed that the ferri/ferro system's reactive impedance is on the order of 40 ohms, whereas the  $\text{RuO}_x$  system's reactive impedance has always been two orders of magnitude less. This fact, pointed out by de Levie (Prof., Georgetown University), prompted us to increase the impedance of our system. We achieved this by decreasing the area of the working electrode. Figure 13 shows the impedance of a  $\text{RuO}_x$  Ti disk of dia 3 mm. The imaginary part of the impedance is now of the order of 100 ohms and the reactance becomes inductive only beyond 5-6 kHz. It was becoming clear at this point that our instrumentation cannot handle the ultra-low impedances of the  $\text{RuO}_x$  and that small phase shifts which would normally be considered error signals, have become equal to the impedance being measured; unless the instrumentation can be improved to reduce these phase shifts, it would be impossible to use this method to study the  $\text{RuO}_x$  system.

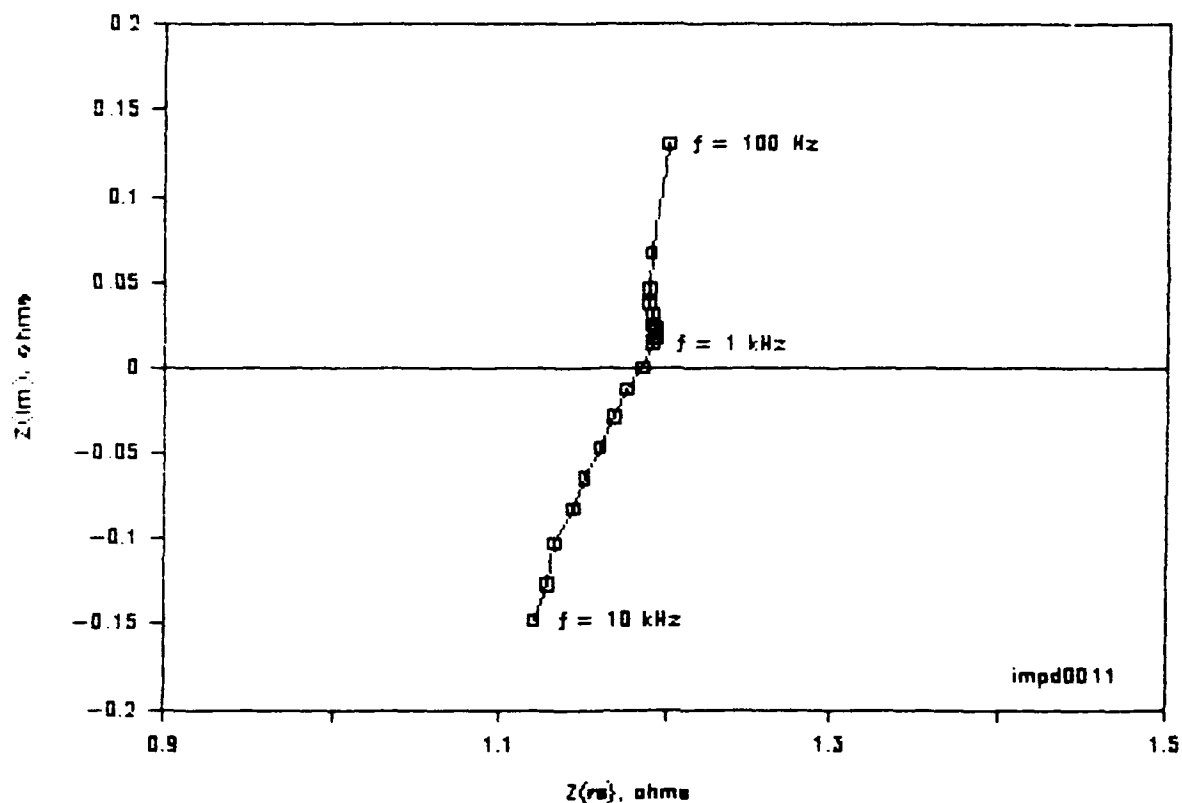


Figure 9. Nyquist Plot for  $\text{RuO}_x$  on a Ti Disk.

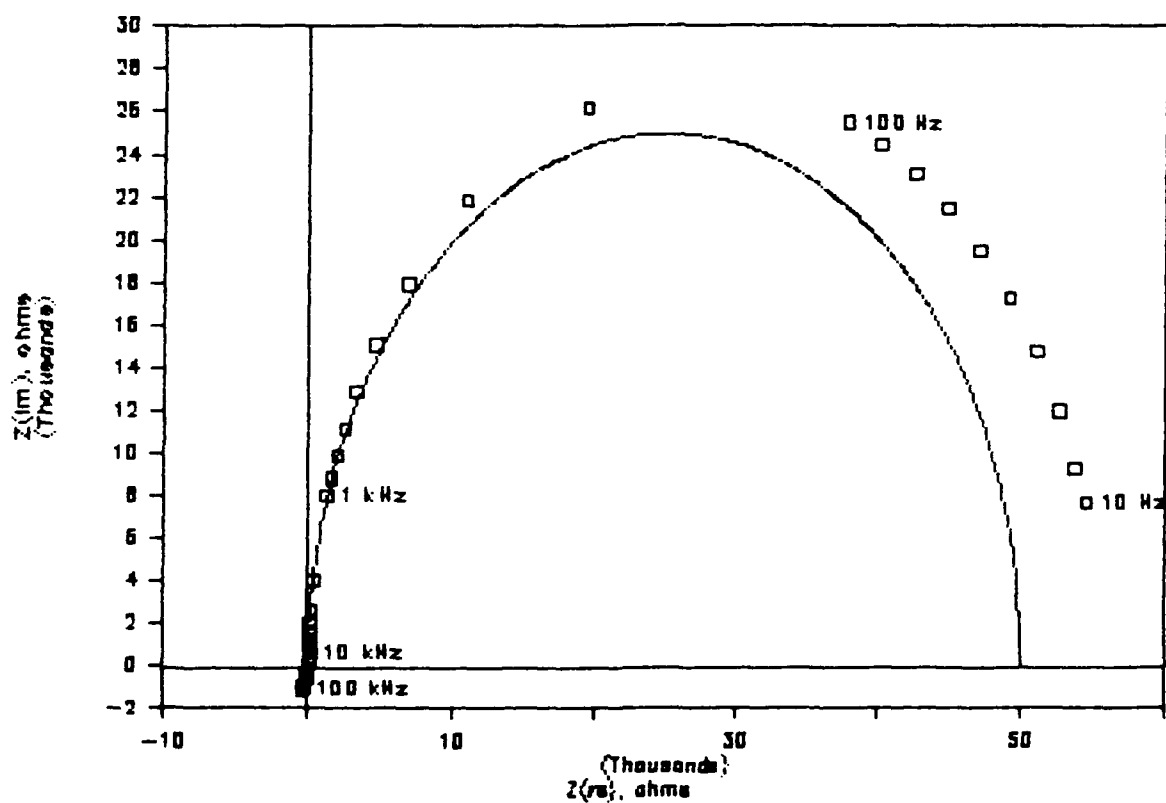


Figure 10. Nyquist Plot for Equivalent Circuit (50 nF Capacitor in Parallel with 50 kΩ Resistor).

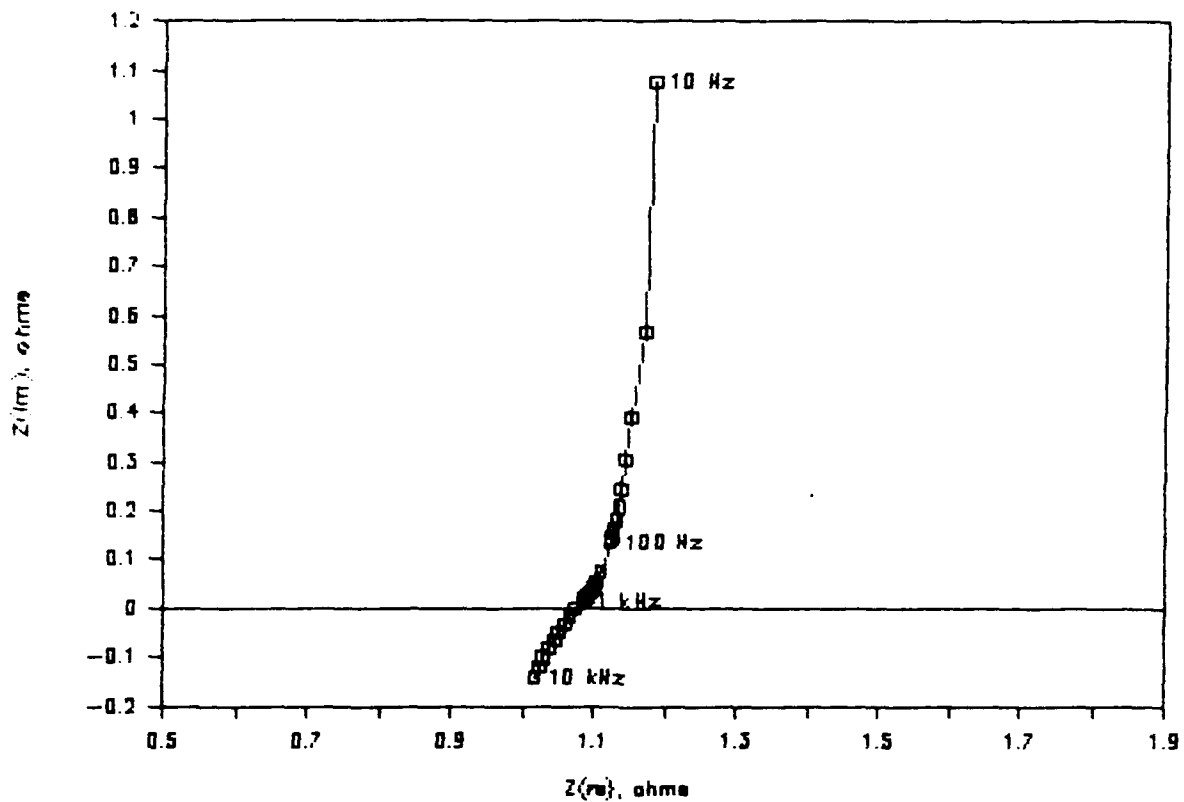


Figure 11. Nyquist Plot for Ferri/Ferro Cyanide Couple.

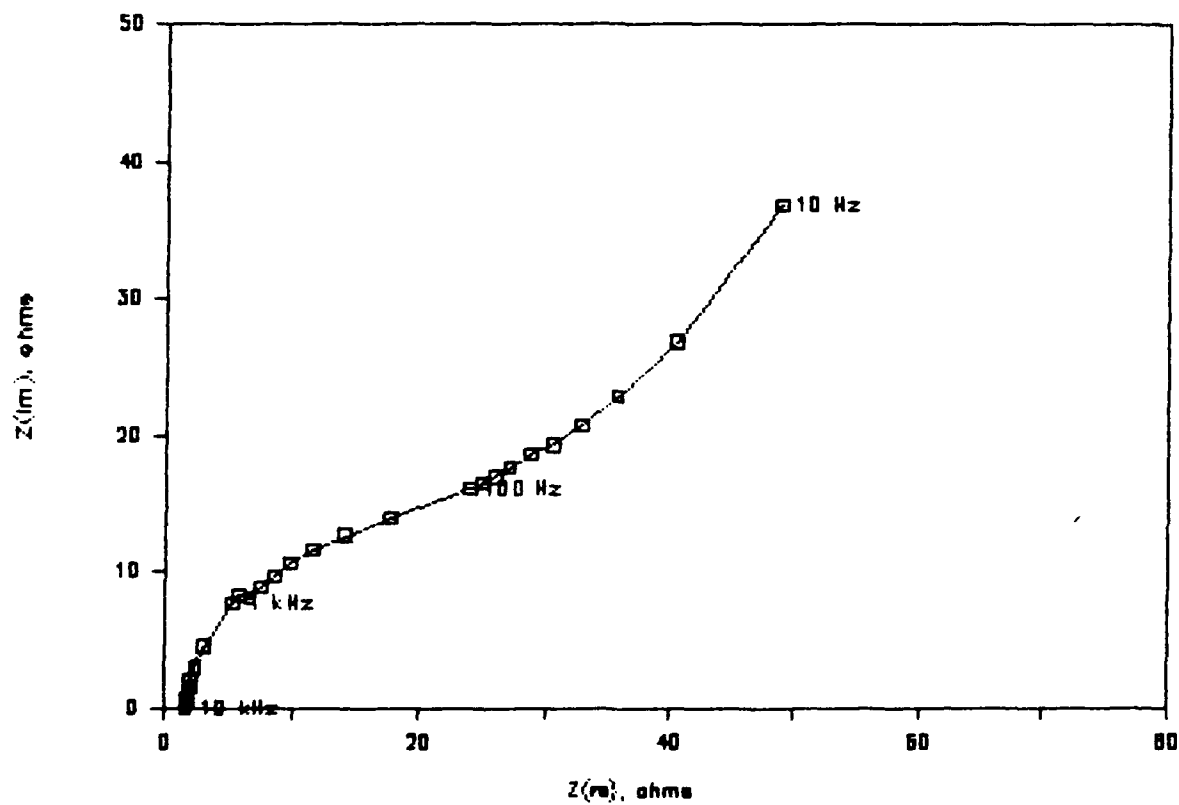


Figure 12. Impedance of Ferri/Ferro Cyanide System.

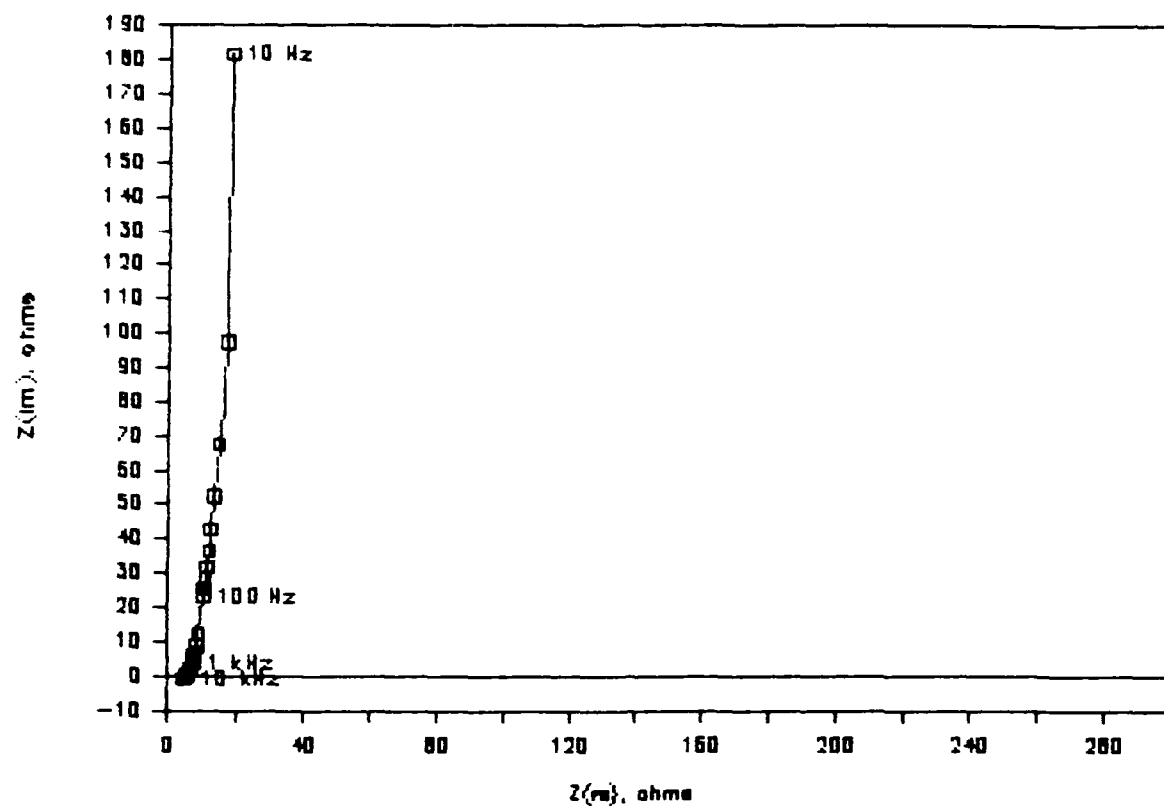


Figure 13. Nyquist Plot;  $\text{RuO}_x$  on Ti Disk of 3 mm Diameter.

#### 4. FUTURE WORK

Based on the SEM and BET surface area results, a closer examination of the  $\text{RuO}_x$  particulates is needed. We will study the particle size of the  $\text{RuO}_x$  using TEM to determine if the particulates possess internal porosity and if this is responsible for specific surface areas greater than  $50 \text{ m}^2/\text{g}$ . Porosimetry will be used to obtain data on pore size distribution.

The evaporation and impregnation methods did not lead to electrodes with significantly higher capacitances compared to an untreated  $\text{RuO}_x$  electrode. One hypothesis is that the evaporation method does not lead to a continuous electrolyte film from the membrane surface to the current collector. We will modify the evaporation method by, for example, painting a  $\text{RuO}_x$ -Nafion mixture on the membrane in order to form a continuous electrolyte film.

Several difficulties were encountered with AC impedance measure methods due to the low impedance of the  $\text{RuO}_x$  electrode. We will examine several alternate strategies for obtaining measurements free from inductive effects.